Available online at www.sciencedirect.com

SciVerse ScienceDirect

Ceramics International 39 (2013) 4377–4381

CERAMICS INTERNATIONAL

www.elsevier.com/locate/ceramint

Effect of the dry nanodispersion procedure in the magnetic order of the Co_3O_4 surface

I. Lorite[a,d,*], L. Pérez[b,c], J.J. Romero[a], J.F. Fernandez[a]

[a]*Instituto de Ceramica y Vidrio, ICV-CISC, 28049 Madrid, Spain*
[b]*Departamento Física de Materiales, Universidad Complutense de Madrid, 28040 Madrid, Spain*
[c]*Instituto de Sistemas Optoelectrónicos y Microtecnología, Universidad Politécnica de Madrid, 28040 Madrid, Spain*
[d]*Universität LeipzigFakultät für Physik und GeowissenschaftenInstitut für Experimentelle Physik II, Linnéstraße 5, 04103, Leipzig, Germany*

Received 1 October 2012; received in revised form 9 November 2012; accepted 9 November 2012
Available online 2 December 2012

Abstract

The ferrimagnetism at the interface of the Co_3O_4 nanoparticles and microparticles used as substrate depends on different parameters of nanoparticles dry dispersion methodology. The quantity of nanoparticles, the energy and the time employed in the process play a key role in the dispersion efficiency. A better dispersion of the nanoparticles produces a larger covering of the Al_2O_3 microparticles substrate and larger UV–vis absorbance and Ms. The magnetic order strongly depends on the number of interaction nanoparticle substrate related to dispersion degree. UV–vis absorbance is a good parameter to measure the dispersion and, therefore, a fingerprint of the magnetic order. Due to the relation between UV–vis absorbance and M_s, it was possible to optimize the dry dispersion parameter to obtain the maximum Ms.

Keywords: Nanodispersion; Co_3O_4; Magnetism

1. Introduction

Solid oxide interfaces are at the forefront of solid-state science and materials research. Interesting properties arise at the interface of two dissimilar transition-metal oxides due to proximity effects [1]. Surface cations are the most sensitive part of these materiales and their relevance increases as materials tend to be nanosized. Nanoparticles have a large specific surface, which provides the presence of a large number of cation than the bulk counterpart. This fuels the search for new fascinating properties at the interface between dissimilar surfaces. In fact, it has been shown that outstanding properties can be obtained as a consequence of the high surface reactivity [2]. Recently, magnetic order has been observed when two non-magnetic oxides are mixed by a simple process. The process is based on a room temperature mechanical dry nanoparticles dispersion by using low energy mixing for a few minutes [3]. Magnetic signal is only shown when dissimilar metal oxide nanoparticles are involved in the mentioned process, but not between materials with the same chemical composition. Therefore, arising of magnetism is ascribed to an interfacial interaction. This phenomena could be related to a solid state charge transference which might be the origin of the recently discovered magnetic signals in oxide multilayers [1] and ceramic mixtures [4]. When cobalt oxide nanoparticles are dispersed on a different metal oxide, the different surface basicity of metals oxides [5] could provide the charge transfer needed to reduce Co^{3+} in octahedral coordination to Co^{2+}, to provide magnetic signal.

The present work studies the role that the different parameters of the dry disppersion (energy and time) in the observed

*Corresponding author at: Universität LeipzigFakultät für Physik und GeowissenschaftenInstitut für Experimentelle Physik II, Linnéstraße 504103 Leipzig, Germany. Tel.: +49 9732756.
E-mail address: lorite@physik.uni-leipzig.de (I. Lorite).

0272-8842/$ - see front matter © 2012 Elsevier Ltd and Techna Group S.r.l. All rights reserved.
http://dx.doi.org/10.1016/j.ceramint.2012.11.025

magnetic ordering. In particular, it is shown how the time and energy of the process can change the magnetic response of the Al_2O_3/Co_3O_4 system.

2. Experimental procedure

Different Al_2O_3/X weight percent Co_3O_4 systems (X is the weight percent of Co_3O_4 nanoparticles employed), hereafter called AlCoX, were produced by dry nanodispersion procedure from α-Al_2O_3 with a purity $>99.99\%$, kindly provided by Vicar, as host microparticles and Co_3O_4 nanoparticles, purchased from Aldrich with a purity $>99.995\%$, as guest nanoparticles. Analytical grade powders were dried at 110 °C for 2 h before the mixing process. All processes were performed avoiding any contact with metal surfaces, such as spatulas or tweezers, to avoid any metallic contamination.

Two different mills were used in the preparation: a shaker turbula type working at 500 rpm with a 60 cm^3 nylon container and alumina balls with different diameters; and a planetary mill working at 200 rpm with a 60 cm^3 alumina container and 15 mm–diameter alumina balls. Alumina was used to avoid magnetic contamination in the mixtures. Different mills and balls were, also, used to study the effect of the energy in the synthesis. The milling time was also varied.

Field emission scanning electron microscopy, was used to study the morphology of the samples (Hitachi S-4700—FESEM). Optical reflectance was measured with a Perkin Elmer spectrophotometer attached with an integrating sphere.

Magnetic properties were measured with a vibrating sample magnetometer VSM (LakeShore) at room temperature.

$CoAl_2O_4$ spinel was prepared by a solid state reaction of a stoichiometric mixture of Co_3O_4 and Al_2O_3. The material was obtained at 1250 °C during 2 h.

The specific surface area was measured by the BET method. The particle size distribution was obtained by a laser granulometer, (Malvern Mastersizer, Quantacrome, Worcestershire, United Kingdom). The average particle size was determined from the cumulative size of the 50% of particles size distribution, d_{50}.

3. Results

Fig. 1 shows the morphology of the two as received powders and the AlCoX, $X=1$ and 10, mixtures. α-Al_2O_3 particles have an average size of $\sim$6 μm with a nearly hexagonal shape (Fig. 1a). Al_2O_3 particles present a flat surface and absence of smaller particles. Co_3O_4 nanoparticles form large agglomerates, Fig. 1c and d show mixtures AlCo1 and AlCo10 respectively, prepared by following the standard treatment, mixer/mill during ten minutes and 1 mm alumina balls. A random dispersion and Co_3O_4 nanoparticles anchoring on the α-Al_2o_3 surface is achieved. The presence of large agglomerates was discarded by an exhaustive FESEM examination of the sample. The sizes of the agglomerates depend on the Co_3O_4 content, i.e. AlCo10 presents a larger proportion of large agglomerates than those in AlCo1, Fig. 1c and d. Micrographs of the dry mixtures with different mixing times and energy are very similar to the one shown and they are not here included for the sake of simplicity. In order to compare, a batch of pure Co_3O_4 was treated following a similar procedure

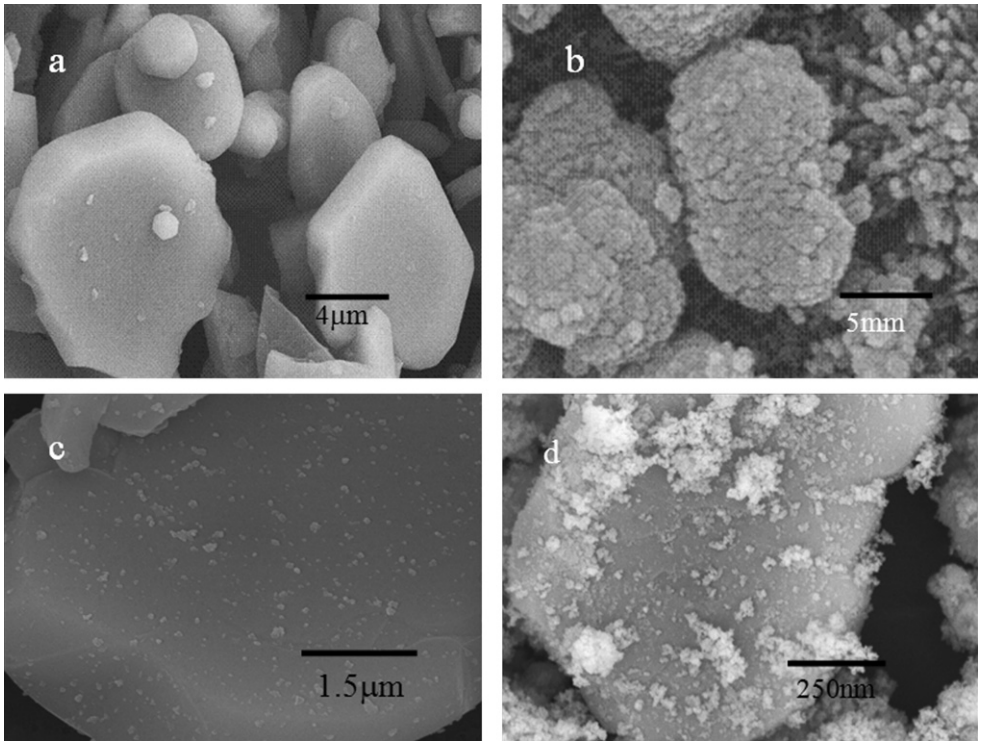

Fig. 1. Electron microscopy of (a) α-Al_2O_3; (b) Co_3O_4 nanoparticles; (c) AlCo1; and (d) AlCo10.

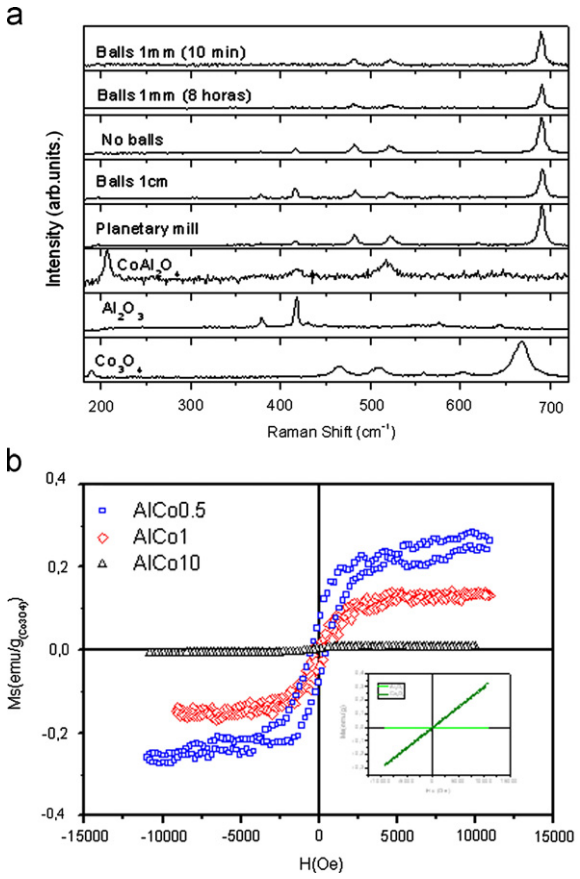

Fig. 2. (a) Raman spectroscopy for the different process of dry nanodispersion AlCoX. For comparison the raw Al_2O_3, Co_3O_4 and $CoAl_2O_4$ are shown, (b) Hysteresis loops measured at room temperature for the mixtures AlCoX. paramagnetic contribution has been subtracted.

and de-agglomeration of the particles was not observed. Hence, the de-agglomeration takes place due to the capability of the nanoparticles to be assembled at the host surface.

Raman spectroscopy was used to rule out the possible formation of different phases during the dry nanodispersion process. Fig. 2a shows the Raman spectra of the samples obtained using different energy in the nanodispersion process. Co_3O_4, Al_2O_3 and the $CoAl_2O_4$ were also measured for comparison. The Raman modes for Co_3O_4 corresponds to $E_g+2F_{g1}+F_{2g}+A_{1g}$ [6]. α-Al_2O_3 has seven Raman actives modes which correspond to $2A_{1g}+5E_g$ [7]. $CoAl_2O_4$ has 4 active modes $3F_{2g}+A_{1g}$ [8]. Only $2F_{2g}$ were observed in our spectra where the most intense is the one at 208 cm^{-1}. For the AlCoX ($X=1$, 10) samples, the Raman modes related to the Co_3O_4 and Al_2O_3, as initial materials, are observed. The anchoring of the nanoparticles to the microparticle substrates must be mediated by an interface interaction between the particles through the hydroxyl groups at the surface of the particles, as previously reported [3].

Magnetic properties at room temperature are compared for two different samples obtained from the standard nanodispersion procedure, AlCo1 and AlCo10. α-Al_2O_3 is paramagnetic at room temperature and Co_3O_4 presents weak T–T antiferromagnetic interaction with the low Neel temperature $T_N=40$ K. Thus, both materials are paramagnetic at room temperature. This paramagnetic contribution has been subtracted in all presented hysteresis loop. From the hysteresis loops shown in Fig. 2b, it can be seen that saturation magnetization is larger in sample AlCo1 than in sample AlCo10. Assuming that the magnetic order is produced by the acid–base interaction between adsorbed OH groups at the dissimilar surfaces, which provides a further redox reaction between the particles [3] to produce the anchoring mechanism, the magnetic signal should be larger in samples with a better dispersion: the better the dispersion the more interaction between OH groups at the dissimilar surfaces.

The largest magnetic signal was provided by the sample AlCo1. Thus, this mixture was obtained by changing the energy and the time of the process to study the magnetic order depending on those parameters.

The energy of the process was changed by using balls of different sizes and by using a planetary mill with balls of 15 mm, also. The energy of the process can be estimated following the results previously published [9]. The energies were ~2 kJ/g and ~10 kJ/g for the processes with alumina balls of 1 cm and 1 mm respectively and 20 kJ/g with the planetary mill. The average size of the Al_2O_3, summarized in Table 1 gives an idea of the energy of each procedure. When no milling balls are used, the energy is clearly smaller than the one produced for the standard process. No changes are observed when using alumina balls of different sizes and a great reduction of the particle and the consequent increase of specific surface area is obtained with the planetary mill, which indicates that the process is clearly more energetic. Planetary mill is a complex process which involves a scissor process that facilitates the size reduction of the microparticles.

Fig. 3 shows the optical and magnetic properties of different mixtures depending on the time and energy of the process. Fig. 3b shows the magnetic properties of the AlCo1 obtained at different energies of the process. Clearly, there is no correlation between the magnetic signal and the energy. Previously, a relationship between the magnetic and the optical absorbance variation was established when Co_3O_4 is dispersed on ZnO [4]. Therefore, it is worthy to study the absorbance for the different samples. Fig. 3a shows the UV–vis Co_3O_4 spectra for samples obtained at different energy. The observed broad bands centered at ~700 and ~400 nm are referred as Co_3O_4 ligand−metal charge transference (LMCT) events which are $O^{2-}\rightarrow Co^{3+}$ and $O^{2-}\rightarrow Co^{2+}$ respectively [10]. There is a clear variation of the absorbance depending on the applied energy in the nanodispersion procedure. α-Al_2O_3 is transparent in the mentioned analyzed wavelength range and thus the absorbance is negligible. Saturation of magnetization can be plotted as a function of the measured absorbance (see Fig. 3c finding a linear relation between both parameters.

The absorbance is related to the dispersion of the nanoparticles. α-Al_2O_3 is UV–vis transparent and presents a low absorbance, but Co_3O_4 nanoparticles have a high absorbance as shown in the inset of Fig. 3d. When the nanoparticles are dispersed over the surface, the absorbance depends on how the particles used as substrate are covered, which is directly related

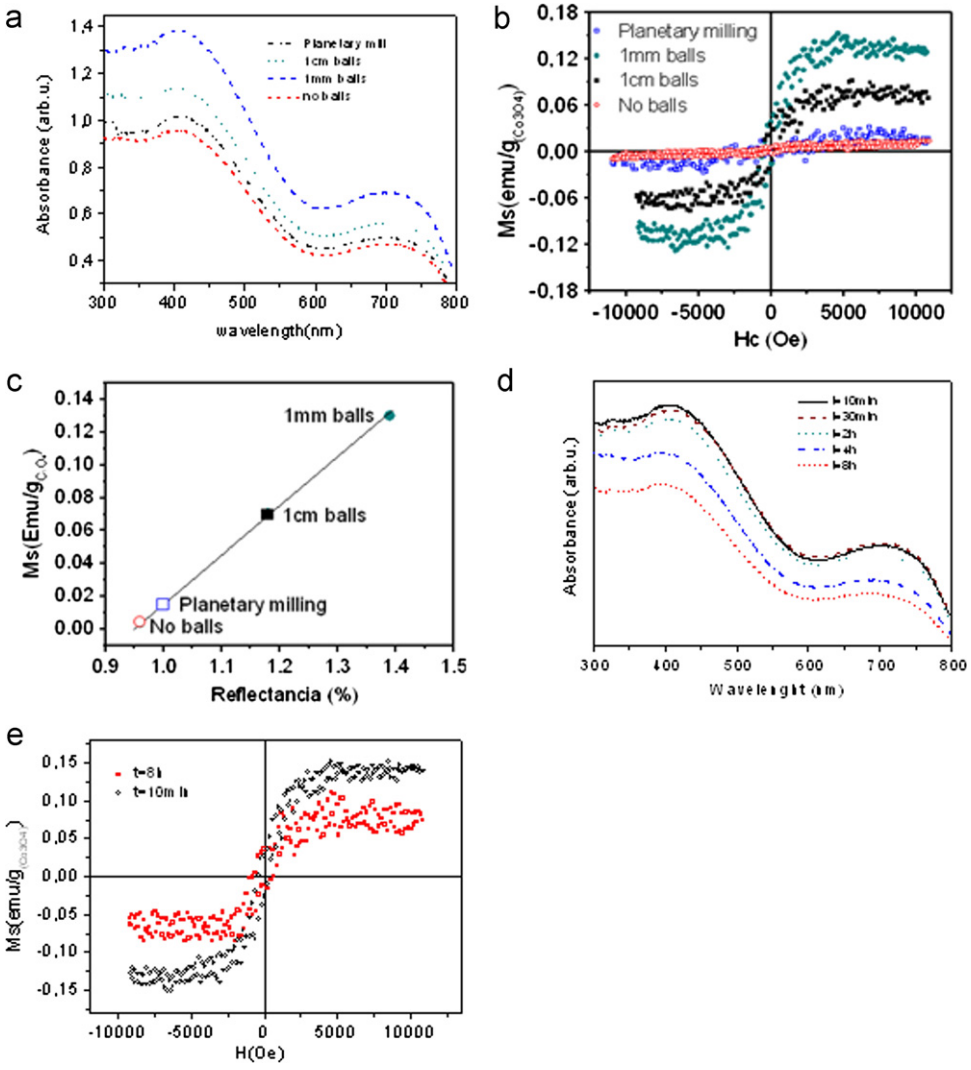

Fig. 3. (a) UV–vis absorbance of the AlCo1 mixtures obtained at different energies. The inset shows the absorbance of the α-Al_2O_3 and Co_3O_4 (b) Hysteresis loops measured at room temperature (c) saturation magnetization as a function of the UV–vis absorbance, (d) UV–vis absorbance of the AlCo1 mixtures obtained by changing the time of the standard dry nanodispersion procedure; (e) hysteresis loops of the mixtures AlCo1 obtained by changing the time of the standard dry nanodispersion procedure.

Table 1
Particle size and specific surface area after different energy milling.

	Initial Al_2O_3	Mixer/mill (balls 1 mm)	Mixer/mill (balls 1 cm)	Mixer/mill (no balls)	Planetary milling
Average particle size	5.90	5.82	5.85	5.96	3.38
Specific surface area	0.5	0.5	0.5	0.5	1

to the dispersion of the nanoparticles over substrate surface. The larger absorbance indicates a better dispersion and therefore a larger number of contacts between dissimilar surfaces to provide magnetic order.

Finally the time of the standard dispersion process was changed between 10 and 8 h. Fig. 3d shows the UV–vis spectra for the different samples obtained. There is a reduction of absorbance with time. This reduction means that the dispersion is more effective as the time of the process is shorter. The magnetic hysteresis loop was acquired for the samples at $t=10$ min and 8 h, Fig. 3e. As expected for the optical measurements, Fig 3a the largest M_s was obtained for the sample at 10 min.

4. Conclusion

Ferrimagnetisms is obtained by a dry nanodispersion of Co_3O_4 nanoparticles over Al_2O_3. The smallest amount of Co_3O_4 in the standard process provides the best dispersion of the nanoparticles. The better the dispersion the more

interactions of nanoparticles/substrate to give rise to the largest M_s. UV–vis absorbance is a good parameter to measure the degree of dispersion and, therefore, a fingerprint of the magnetic order.

The energy of the process and also the time can change the effectiveness of the dry nanodispersion, as seen from the UV–vis absorbance reducing the magnetic order in comparison with the standard dispersion.

Acknowledgments

This work was supported by projects MAT2010-21553-C02-01, MAT2011-28751-C02-02 and partially supported by the Sonderforschungsbereich under Grant no. SFB 762, "Functionality of Oxide Interfaces."

Magnetic measurements have been carried out at CT-ISOM funded by the Spanish Ministerio de Ciencia e Innovación.

References

[1] M.A. García, M.L. Ruiz-González, A. Quesada, J.L. Costa-Krämer, J.F. Fernández, S.J. Khatib, A. Wennberg, A.C. Caballero, M.S. Martín-González, M. Villegas, et al., Interface double-exchange ferromagnetism in the Mn–Zn–O system: new class of biphase magnetism, Physical Review Letters 94 (2005) 217206.

[2] A. Brinkman, M. Huijben, M. van Zalk, J. Huijben, U. Zeitler, J.C. Maan, W.G. van der Wiel, G. Rijnders, D.H.A. Blank, H. Hilgenkamp, Magnetic effects at the interface between non-magnetic oxides, Nature Materials 6 (2007) 493.

[3] Marisol Martin-González, Miguel A. García, I. Lorite, José L. Costa-Krämer, A.Fernando Rubio-Marcos, C.N. Carmona, José F. Fernándezc, A solid-state electrochemical reaction as the origin of magnetism at oxi de nanoparticle interfaces, Journal of the Electrochemical Society 157 (3) (2010) E31–E35.

[4] M.A. García, F. Jiménez-Villacorta, A. Quesada, J. de la Venta, N. Carmona, I. Lorite, J. Llopis, J.F. Fernández, Surface magnetism in ZnO/Co_3O_4 mixtures, Journal of Applied Physics 107 (2010) 043906.

[5] J.A. Duffy, Optical basicity of a solid oxide, Geochimica Cosmochimica Acta 57 (1993) 3961.

[6] J. Jiang, L. Li, Synthesis of Sphere-like Co_3O_4 nanocrystals via a simple polyol route, Materials Letters 61 (2007) 4894.

[7] R.S. Krishnan, Raman spectrum of alumina and the luminescence and absorption spectra of ruby, Nature 160 (4053) (1947) 26.

[8] L.D. Kock, D. De Waal, Raman studies of the underglaze blue pigment onceramic artefacts of the Ming dynasty and of unknown origins, Journal of Raman Spectroscopy 38 (2007) 1480.

[9] W. Pei-zhong, Q. Xiao-hong, Q. Ying-huai, Xuan-hui, Energy analysis of mechanical alloying of molybdenum disilicide in a new-type high energy vibrating ball mill, Journal of China University of Mining and Technology 18 (2008) 0449–0453.

[10] R. Xu, H. Chun Zeng, Self-generation of tiered surfactant superstructures for one-pot synthesis of CO_3O_4 nanotubes and their close- and non-close-packed organizations, Langmuir 20 (2004) 9780–9790.